Synergistic Effect of Hierarchically Porous 4A Zeolite on Improving the Fire Retardancy and Reducing the Fire Toxicity of Ammonium Polyphosphate Treated Wood Composites

Shaodi Zhang,[a,c] Yuhui Wu,[a,c] Xi Guo,[a,c] Haiying Shen,[a,c] Mingchang Zhang,[a,c] and Mingzhi Wang [a,b,c,∗]

The synergistic effect of hierarchically porous zeolites on the fire retardancy and fire toxicity of ammonium polyphosphate (APP) treated wood composites was studied in this work. Hierarchically porous 4A (H4A) zeolite and 4A zeolite were hydrothermally synthesized and characterized. Several groups of wood composites containing APP as fire retardant and H4A/4A zeolites as synergists were fabricated. Thermogravimetric (TG) results showed that H4A zeolite increased the char formation and enhanced the thermal stability of APP treated wood at higher temperature. Cone calorimetry test results suggested that H4A zeolite reduced the heat release rate (HRR) and decreased CO produce rate (COPR) of APP treated wood composites. Moreover, H4A also exhibited better smoke suppression than 4A zeolite when the APP content was small. These results demonstrated that H4A zeolites may be a promising synergistic component for improving the fire retardancy and reducing the fire toxicity of APP treated wood composites.

INTRODUCTION

Wood composites have become a prevalent construction engineering material due to their low density and good mechanical properties (Wang *et al.* 2014a). However, the cellulose, hemicellulose, and lignin content of wood composites are flammable; the danger of heavy economic loss and casualties restricts composite application in dwellings and other buildings (Lowden and Hull 2013).

Wood composites can be chemically modified with fire retardants. Ammonium polyphosphate (APP) and ammonium dihydrogen phosphate (ADP) were typically used as fire retardants of wood owing to their eco-friendly properties compared with halogen fire retardants (LeVan 1984; Diniz 2010; Jiang *et al.* 2010; Lowden and Hull 2013; Jiang *et al.* 2015). APP can decompose to polyphosphoric acid when heated, and the acid catalyzes the dehydration of cellulose and increase the production of char residue of wood. The residue acts as a protective layer to prevent the emission of combustible gases and the impregnation of oxygen. Thus, the propagation and intensity of fire can be restrained. However, toxic gases including CO are emitted due to the incomplete combustion of wood (Wang *et al.*

2014b; Yan *et al.* 2017), which leads to heavy casualties or long-term damage in humans (Stec and Hull 2010). Furthermore, smoke production increases dramatically when a high concentration of APP solution (>15%) is used. Because smoke reduces visibility and impedes escape from fire, the inhibition of smoke is just as vital as CO (Naeher *et al.* 2007). Therefore, the modification of the APP fire-retardant system is urgently required to improve the fire-retarding efficiency and to reduce toxicity during fire. Inorganics such as zeolites have been applied as synergists of fire retardants to solve these problems, with positive results (Demir *et al.* 2005; Lin *et al.* 2011).

Zeolites are crystalline aluminum silicates, comprised of aluminum and silicate oxygen tetrahedral through corner sharing, giving rise to a three-dimensional framework with intracrystalline microporous structures (Breck 1974). As nanoscale porous materials, zeolites exhibit superior catalytic property, size or shape selectivity, and absorbability; they have become increasingly important in many industrial applications, *e.g.*, in automotive catalysis, sewage purification, and petroleum processing (Zorpas *et al.* 2000; Vermeiren and Gilson 2009; Wang *et al.* 2011; Deka *et al.* 2013). There are many types of zeolites, and they are named LTA, FAU, ZSM-5, *etc.*, based on the framework structure and channel type. LTA type zeolites have a three-dimensional, 8-ring channel system. The typical pore size of synthesized LTA zeolites is 4 Å (0.4 nm), so it is known also as 4A zeolite. Previous researchers have also clarified the efficiency of microporous 4A zeolite by improving the fire retardancy of APP treated materials. Fire toxicity was inhibited in multiple studies. Bourbigot *et al.* (1996) added 4A and other zeolites into the intumescent (APP)-pentaerythritol (PER) system treated polymers, resulting in a great improvement in the fire retardant properties; the presence of zeolites increased the thermal stability of materials at high temperatures. Wang *et al.* (2015) found that 4A zeolite catalyzes the thermal degradation of APP treated wood-plastic composites, leading to the formation of a more stable and compact char layer, and gas/solid-phase fire retardancy mechanisms of zeolites were also speculated. Wang *et al.* (2014b) treated plywood with APP and 4A zeolite and investigated the combustion behavior of obtained plywood by cone calorimetry. The heat release and emission of CO were decreased by the APP/4A system. In a recent study, different zeolites were used to modify the fire retardant coating of wood, and the results indicated that the FAU type 13X zeolite with larger pore size exhibited better smoke suppression properties than the 4A zeolite (Wu *et al.* 2017). In summary, zeolite catalyzes char formation and enhances the strength of a char layer to prevent wood from oxygen, and the special porous structure may act as a physical barrier to limit the transfer of heat and reduce the production of toxic gases through absorption and catalytic property.

The small aperture size (ranging from 3 to 15 Å) and relatively long transport path of microporous zeolites may cause mass transport limitations, leading to the weakening of its catalytic and absorptive performance. These drawbacks have also restrained the application of microporous zeolites in other fields like the conversion of biomass. To overcome these shortages, research efforts have focused on introducing mesopores into zeolites, including the attempts of mesoporous zeolites and the synthesis of hierarchically porous zeolites (Choi *et al.* 2006; Pérez-Ramírez 2012; Ates *et al.* 2015; Gamliel *et al.* 2016). In particular, hierarchically porous zeolites contain both micro- and mesoporosity and have shown better mass transport performance and improved catalytic efficiency than microporous zeolites (Gueudré *et al.* 2014; Fu *et al.* 2015; Besser *et al.* 2016). However, the topic of synergistic effect of hierarchically porous zeolites on fire retardancy of fire retardant-treated wooden materials has not been reported yet, and this may be of considerable significance for improving the fire retardancy of wood or other lignocellulosic

materials and reducing fire casualties.

In this work, hierarchically porous 4A (H4A) and 4A zeolite were hydrothermally synthesized. Dimethyloctadecyl[3-(trimethoxysilyl)propyl]ammonium chloride (DTPAC) was used as a template to introduce intracrystalline mesoporous into the framework of 4A zeolite to obtain H4A zeolite. Several groups of wood composites containing APP as fire retardant and H4A/4A zeolites as synergists were fabricated. The fire retardancy and fire toxicity of APP treated wood composites were assessed by thermogravimetric (TG) analysis and cone calorimetry.

EXPERIMENTAL

Materials

Dimethyloctadecyl[3-(trimethoxysilyl)propyl]ammonium chloride (DTPAC, 60 wt% in methanol) was purchased from Beijing Bailingwei Technology Co. Ltd. (Beijing, China). Analytical grade reagents for the synthesis of zeolites including sodium hydroxide (NaOH), sodium aluminate ($NaAlO_2$), and sodium metasilicate nonahydrate ($NaSiO_2 \cdot 9H_2O$) were provided by local companies in China.

Ammonium polyphosphate (APP, average polymerization degree: n > 1000) was purchased from Ji'nan Taixing Fine Chemical Co., Ltd. (Jinan, China). Wood flour of poplar (W, *Populus tomentosa*, particle size between 20 to 60 mesh sieve) was provided by Gaocheng Xingda Wood Flour Company (Hebei, China), and dried in an oven at 103 °C for 8 h prior to usage. The phenol-formaldehyde (PF) resin adhesive was synthesized by batch copolymerization using phenol and formaldehyde with a molar ratio of 1:2.2, following the reported method (Li *et al.* 2017). The solid content of the resin was 45%, the viscosity was 100 to 150 mPa s, with a pH of 11 to 12. The distilled water used in this work was self-made in the lab.

Synthesis of H4A/4A Zeolite

H4A zeolite was prepared according to published procedures (Choi *et al.* 2006). First, 1.2 g of NaOH and 30.0 g of distilled water were added to a 500 mL polypropylene flask and stirred until a clear solution was prepared, and 8.2 g of $NaAlO_2$ was dissolved in the NaOH solution (solution A). Subsequently, 28.4 g of $NaSiO_2 \cdot 9H_2O$ was dissolved in 69.1 g of distilled water in another 500 mL polypropylene flask, and 3.3 g of DTPAC was added into the $NaSiO_2 \cdot 9H_2O$ solution while stirring to obtain solution B. Solution B was added to solution A, leading to the formation of a gel having the mole composition of $1Al_2O_3$:$3.3Na_2O$:$2SiO_2$:$128H_2O$:0.08 DTPAC. The gel was stirred by a blender for 2 h until a homogeneous mixture was obtained. The mixture was heated in a water bath with electromagnetic stirring for 4 h at 95 °C; the crystallization process of target zeolite occurs in this procedure. After it was vacuum filtered with distilled water for 4 times, the crystallized zeolite was oven-dried at 110 °C for 3 h and calcined in an air atmosphere at 550 °C for 6 h in a muffle furnace to remove DTPAC. The mesoporosity was introduced into the zeolite particle through the calcination process.

For the synthesis of 4A zeolite, solutions A and B were prepared following the same procedure mentioned above, except that DTPAC was not added in solution B, and the mixture of solution A and B was stirred in a polypropylene flask for 2 h at room temperature, then heated at 100 °C for 4 h in an oven. The product was also filtered and dried like H4A zeolite but did not undergo the calcination.

The synthesized zeolites were milled to powder to break up aggregates.

Characterization of H4A/4A Zeolite

Powder X-ray diffraction (XRD) patterns were acquired with Cu Kα radiation at 40 kV and 40 mA (Bruker, D8 ADVANCE, Billerica, MA, USA). The data were recorded in the 2θ range of 5 to 50° with an angular step size of 0.02° and a counting time of 8 s per step. The morphology of zeolites was obtained by field emission scanning electron microscope (FE-SEM; SU8010, HITACHI, Chiyoda, Tokyo, Japan). The N$_2$ adsorption/desorption isotherms were determined using an automated physisorption analyzer (BEL max 00097, BEL, Bengaluru, India) at -196 °C. The samples were activated by removing the water of hydration at 350 °C under 10^{-4} Pa before the adsorption measurement. The pore size distributions were calculated by the Barrett-Joyner-Halenda (BJH) method using the adsorption branch for the mesopores analysis.

Thermogravimetric Analysis

Poplar wood flour (60 mesh) was blended with APP and/or zeolites in different ratios, as shown in Table 1. TG analysis was carried out in a thermogravimetric analyzer (TGA Q50 V20.10 Build 36, TA instruments, New Castle, DE, USA) using a heating rate of 10 °C ·min^{-1} up to 800 °C under air atmosphere (79% of nitrogen and 21% of oxygen).

Preparation of Wood Composites

Six groups of wood composites were fabricated. The wood flour with particle sizes of 20 to 60 meshes were blended with APP and/or zeolites by different combination ratios, as shown in Table 1. PF resin adhesive (10 % of wood flour weight) was manually blended in the mixture, which was then compressed in a mould. The semi-finished slabs were hot-pressed under 1.8 to 2.5 mPa pressure at 150 °C for 10 min. The fabricated wood composites panels were cut into specimens of 100 mm × 100 mm × 10 mm dimensions for cone calorimetry.

Table 1. Combinations and Ratios of Different Samples for TG Analysis and Cone Calorimetry

Group	W	W + APP	W + 4A	W + H4A	W + APP + 4A	W + APP + H4A
Ratio	-	APP: 10% (of W weight)	4A:10%	H4A: 10%	APP: 6.7% 4A : 3.3%	APP: 6.7% H4A : 3.3%
The addition of PF resin adhesive (solid content) was 10% of W for all groups.						

Cone Calorimetry

Cone calorimetry is a standard method for burning materials with specified dimensions under a constant heat flux to observe the combustion behavior. It can simulate the fire environment precisely and has been widely used in the field of wood fire retardants (Steen-Hansen and Kristoffersen 2007; Kim *et al.* 2012). A cone calorimeter (FTT00007, East Grinstead, UK) was used with an external heat flux of 50 kW·m^{-2}, according to the ISO 5660 standard (2015). The data gathered to investigate the combustion properties of wood composites included heat release rate (HRR), total heat release (THR), smoke produce rate (SPR), total smoke production (TSP), and CO produce rate (COPR).

bioresources.com

RESULTS AND DISCUSSION

Characterization of Zeolites

The FE-SEM images of 4A and H4A zeolites are presented in Fig. 1. The 4A zeolite exhibited regular cubic shape with glazed surfaces. The H4A zeolite showed a distinct change in morphology; homogeneous and globular particles in the range of 2 to 3 μm with rugged surfaces were observed.
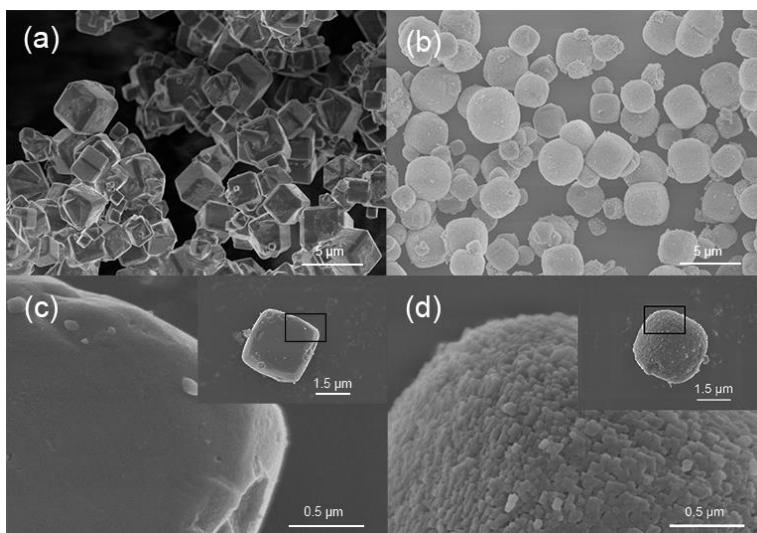
Fig. 1. FE-SEM images of 4A and H4A zeolites. (a), (b) are FE-SEM images of 4A zeolite with magnification of 4 k and (c), (d) are for H4A zeolite with magnification of 50 k. The inset of (c) and (d) showed the morphology of singular particles and the region that has been magnified was marked by a rectangle.
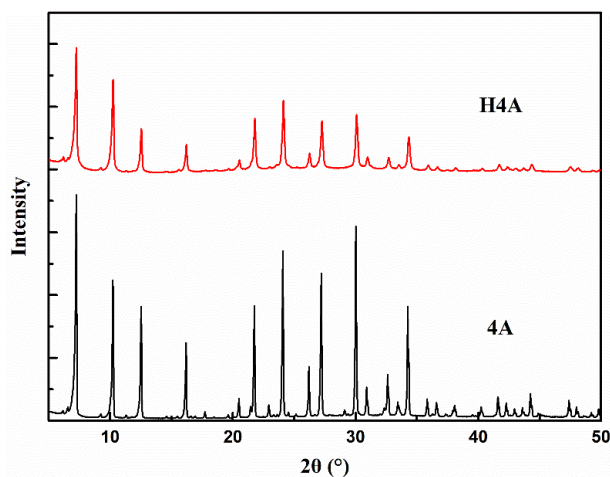
Fig. 2. XRD patterns of H4A and 4A zeolites synthesized in this study

Figure 2 reveals the XRD patterns of samples. Both 4A and H4A zeolites showed characteristic peaks of LTA type zeolites (Treacy and Higgins 2007), suggesting that crystalline LTA type zeolites were successfully synthesized. The only difference was a slight decrease in the intensity of the diffraction peak, indicating that the size of the crystalline domain of H4A zeolite was decreased because of the DTPAC addition (Cho *et al.* 2009).
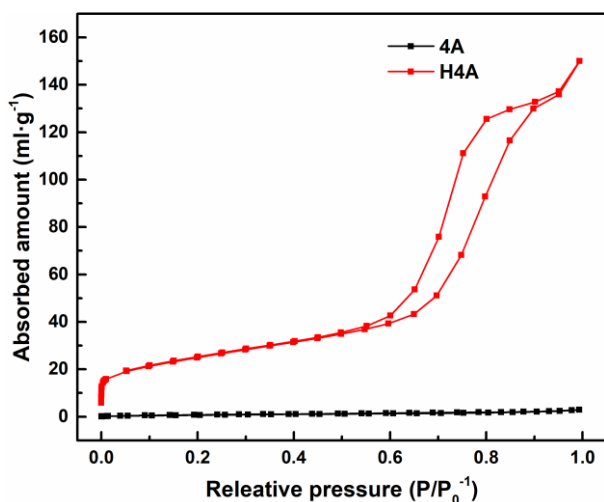
Fig. 3. N$_2$ adsorption/desorption isotherms of H4A and 4A zeolite; the H4A zeolite show a typical type-IV isotherm.

The N$_2$ adsorption/desorption isotherm of H4A zeolite presents a typical type-IV isotherm, according to Fig. 3. The pore size analysis by the BJH algorithm gave a sharp distribution of mesopores centered at around 10.0 nm (Fig.4), indicating that the mesoporosity was introduced into H4A zeolite successfully.
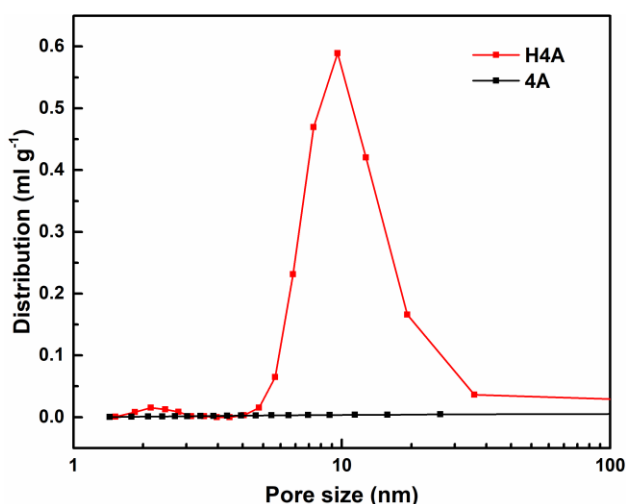
Fig. 4. The pore size distribution of H4A and 4A zeolites

TG Analysis

Figures 5 and 6 show the TG and derivative thermogravimetry (DTG) curves of different samples. The results are summarized in Tables 2 and 3. The thermal degradation of wood can be divided into three stages, as shown in TG and DTG curves. Wood (W) starts to absorb heat at first. The water evaporates under 135 °C, and about 3.8% of the mass was lost during this process (Table 2). The second stage at 135 to 375 °C corresponds to the decomposition of wood, including the dehydration, rearrangement, and pyrolysis of cellulose, hemicellulose, and lignin. Approximately 67.9% of mass was lost, and the mass loss rate reached the maximum value (R_{1max}: 0.0087%·°C^{-1}) at T_{1max} of 320 °C (Table 3).

Some stable char remained during this process (Yunchu *et al.* 2000). With the temperature increasing, the third stage occurred at around 380 to 500 °C, when the char was oxidized and approximately 4.7% of residue was retained at 800 °C.
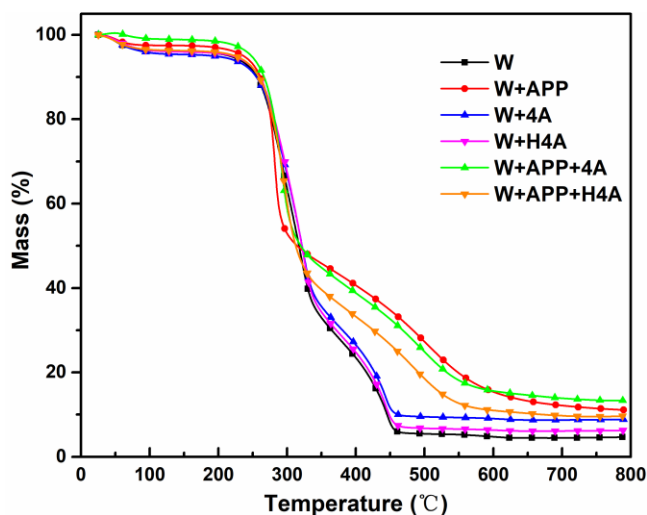
Fig. 5. TG curves
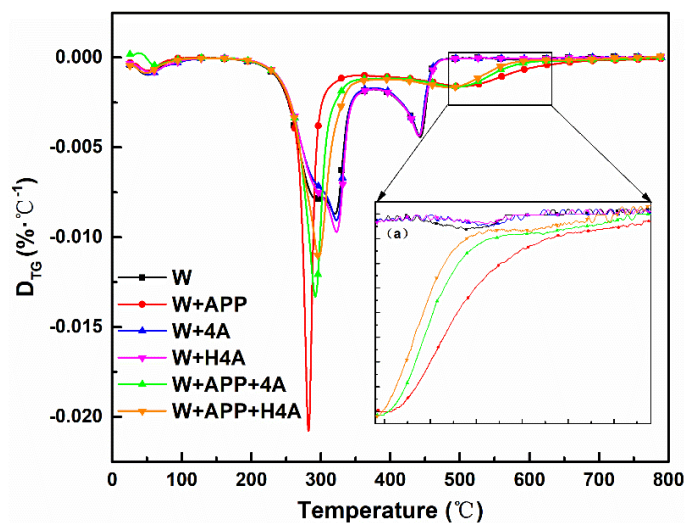
Fig. 6. DTG curves, (a) Enlarged detail of the 500 °C to 800 °C region

The residues of both W + 4A (8.9%) and W + H4A (6.3%) were higher than that of W. Metal cations have a strong effect on pyrolysis of cellulose and could increase the formation of char, *e.g.*, the Na^+ within the framework of zeolites (Soares *et al.* 1998). More residue demonstrates that the sample is more thermal-stable, which suggests that the fire retardancy had been improved (Rowell 1984). Another plausible explanation is that the solid-acidity of zeolites exhibits similar catalytic performance to phosphoric acid (Moreno-Recio *et al.* 2016).

Table 2. TG Analysis Data of Different Samples under Air Atmosphere

Group	First Stage		Second Stage		Third Stage		Residue (%)
	Range (℃)	ML (%)	Range (℃)	ML (%)	Range (℃)	ML (%)	
W	30-135	3.7	135-377	68.0	377-500	23.5	4.7
W + APP	30-122	2.5	122-356	52.2	356-750	34.1	11.1
W + 4A	30-142	4.6	142-380	65.3	380-500	21.3	8.9
W + H4A	30-138	3.9	138-376	66.8	376-500	22.9	6.3
W + APP + 4A	30-150	1.1	150-395	59.3	395-700	26.2	13.3
W + APP + H4A	30-162	3.6	162-395	61.9	395-700	24.6	9.7
ML represent the mass loss in each stage. Residue are the residue remained at 800 ℃.							

Table 3. DTG Data of Different Samples under Air Atmosphere

Group	R_{1max} (%·℃$^{-1}$)	T_{1max} (℃)	R_{2max} (%·℃$^{-1}$)	T_{2max} (℃)
W	0.0087	320	0.0044	442
W + APP	0.0207	282	0.0016	498
W + 4A	0.0091	322	0.0044	441
W + H4A	0.0097	322	0.0043	441
W + APP + 4A	0.0133	292	0.0016	499
W + APP + H4A	0.0110	298	0.0017	487
R_{1max} and R_{2max} denote the mass loss rates of the first and the second mass loss peak, respectively. T_{1max} and T_{2max} are the temperature at which the first and the second mass loss peak occurs, respectively.				

Less residue remained from W + APP + H4A/4A than that of W + APP due to the reduction of APP content, as shown in Table 2. APP is the main driver in improving fire retardancy. However, the combination of APP and zeolites showed excellent synergistic effects in other aspects. In the second stage, the R_{1max} of W + APP + H4A and W + APP + 4A was much smaller than that of W + APP, and the T_{1max} of W + APP + H4A was 298 ℃, 16 ℃ higher than that of W + APP. Thus, the unique porous structure of H4A zeolite could enhance the thermal stability of wood. In the third stage, the initial decomposing temperature of W + APP was 356 ℃, which increased to 395 ℃ for W + APP + H4A/4A (Table 2). The DTG curves of W + APP + H4A/4A were lower than that of W + APP after 500 ℃ (inset of Fig. 6), especially for W + APP + H4A, which means that the remaining char was more thermally stable at a higher temperature.

These results indicated that H4A zeolite increased the char residue at a low content of APP and also improved the thermal stability of the wood and the char by catalyzing the formation of an intercalated network, leaving Si-O-P and P-O-C bonds in the char (Wang *et al.* 2015; Yan *et al.* 2017).

bioresources.com

Cone Calorimetry Test

Heat release

Heat release rate is a critical parameter for evaluating fire intensity and the velocity of fire propagation. The HRR curves of samples are illustrated in Fig. 7, and the data are listed in Table 4. Wood showed two heat release peaks during the combustion process. The first heat release peak corresponded to the burning of volatile gases produced by the pyrolysis of surface wood. After the pyrolysis of surface wood and the combustion of volatile gases, a protective char layer was generated, such that the heat transfer was slow and pyrolysis was inhibited. Subsequently, the char layer cracked, and the under-layer substrates began pyrolysis. More combustible volatiles escaped, leading to the appearance of the second peak (Spearpoint and Quintiere 2000; Marney and Russell 2008). The HRR declined sharply and reach a plateau, due to the formation of carbonaceous residue and the gradual extinguishment of the fire.
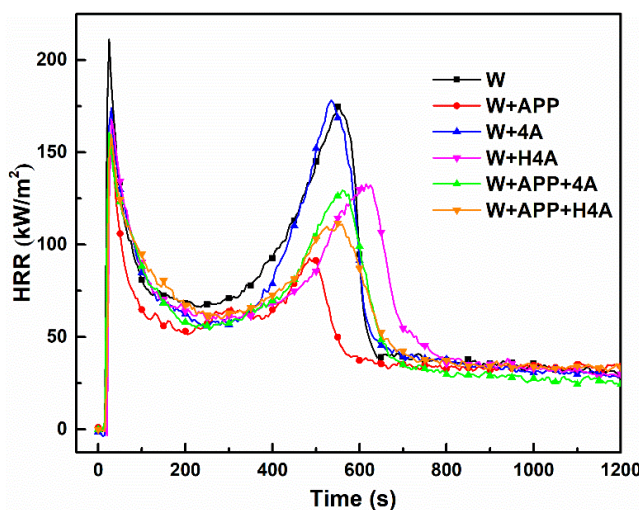
Fig. 7. The heat release rate (HRR) curves of different treated samples

Both $pHRR_1$ and $pHRR_2$ of W + APP were lower than those of W (26% less for $pHRR_1$ and 47% less for $pHRR_2$). The first peak represents the combustion of flammable gases produced by the degradation of wood. APP inhibited wood combustion effectively by releasing NH_3 to dilute the combustible gases and by promoting the char formation to restrain the emission of heat, as discussed previously. The second peak of W + APP appeared earlier (485 s) than that of W (550 s) but was deferred with the further addition of H4A. This result suggests that the thermal stability of the char layer of W + APP + H4A is enhanced due to the formation of Si-O-P and P-O-C bonds within the structure.

The first heat release peaks of zeolite treated samples (W + 4A/H4A, W + APP + 4A/H4A) were all decreased, as shown in Fig. 7 and Table 4. Zeolites can release H_2O to dilute the flammable gases, and its framework will act as a barrier to restrain the transmission of heat and O_2 to inhibit wood combustion (Wang *et al.* 2015). The second peak ($pHRR_2$) of W + 4A was increased slightly and occurred 15 s earlier than that of W. In contrast, for W + H4A, the $pHRR_2$ of W + H4A declined to 132.73 $kW \cdot m^{-2}$ and was delayed from 550 s for W to 615 s. This result clarified that the unique framework of H4A zeolite makes the structure denser and more difficult to crack. Accordingly, H4A zeolite exhibited better performance in reducing the heat release compared with 4A zeolite with 10 wt% of fire-retardant.

Table 4. Results of Cone Calorimetry Test of Different Samples

Group	pHRR$_1$ (kW·m^{-2})	T_1 (s)	pHRR$_2$ (kW·m^{-2})	T_2 (s)	THR (kW·m^{-2})	TSP (m^2·s^{-1})	COY (kg·kg^{-1})
W	211.29	25	174.54	550	91.86	52.20	0.045
W + APP	156.47 (26%)	30	92.75 (47%)	485	59.60	16.64 (68%)	0.054
W + 4A	173.99 (18%)	30	178.22 (-2%)	535	77.73	31.45 (40%)	0.022
W + H4A	167.72 (21%)	30	132.73 (24%)	615	75.81	23.14 (56%)	0.023
W + APP + 4A	160.82 (24%)	25	129.21 (26%)	560	70.25	38.15 (27%)	0.023
W + APP + H4A	159.54 (24%)	30	111.71 (36%)	550	65.85	22.25 (57%)	0.025

The pHRR$_1$ and pHRR$_2$ represent the value of the first and second heat release peak. T_1 and T_2 are the time at which the heat release peak occurs. THR is the total heat release and TSP is the total smoke production. COY is the CO yield of different specimens during the test. The percentage in the parentheses represent the decreasing amount compared with W.

Smoke production

Because smoke reduces visibility and impedes escape from fire, it is a principal cause of fire casualties (Naeher *et al.* 2007). Smoke release rate (SPR) and total smoke production (TSP) are thus crucial parameters. Figure 8 shows the SPR curves of different samples, and TSP values are listed in Table 4. Smoke was released rapidly at around 450 s to 700 s, which was attributed to the glowing combustion and further burning of under-layer wood. Accordingly, the smoke production was mainly affected by the coherence and thermal stability of char layer. The SPR curves of treated samples were all lower than W, as shown in Fig. 8. This result suggested that treated wood produces more coherent and thermal-stable char layers. Although the TSP of W + APP was only 16.64 $m^2 \cdot s^{-1}$, 68% less than W when the ratio of APP was only 10%, it would have increased dramatically if APP was more than 15%, as shown in earlier research (Wang *et al.* 2014b). H4A and 4A zeolites exhibited obvious differences in the reduction of smoke. The TSP were 31.45 $m^2 \cdot s^{-1}$ and 38.15 $m^2 \cdot s^{-1}$ for W + 4A and W + APP + 4A, while the TSP of W + H4A and W + APP + H4A were 23.15 $m^2 \cdot s^{-1}$ and 22.25 $m^2 \cdot s^{-1}$, respectively, as shown in Table 4. The SPR curves of H4A treated samples with or without APP were also much lower than those of 4A treated ones. Thus, H4A zeolite may strengthen the char layer by making it compact. Therefore, the smoke could not pass through, and it might also absorb the solid particles and droplets of smoke due to the presence of mesopores (as indicated in the N_2 adsorption/desorption isotherms and pore size distribution, Fig. 3 and Fig. 4).
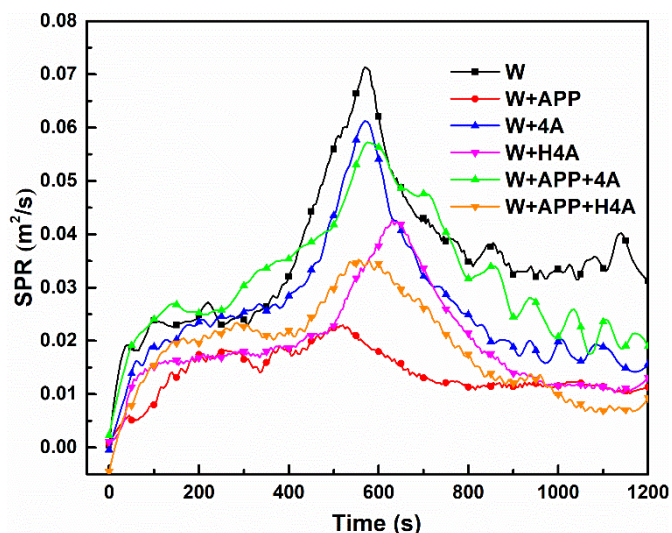
Fig. 8. The smoke production rate (SPR) curves of different treated samples

CO production

The toxicity of gases is a cause of casualties during fire (Stec and Hull 2010). Carbon monoxide (CO) is emitted when wood burns incompletely. The CO production rate (COPR) is shown in Fig. 9, and the COY of different samples is given in Table 4. The COPR of W exhibited two peaks, corresponding to the flame combustion of surface wood and glowing combustion of the char layer, respectively, as shown in Fig. 9. The second peak of COPR of W was delayed from 570 s to around 620 s and was lowered when H4A was added (Fig. 9, W + H4A).

For W + APP, the second peak was shifted to 200 s to 400 s, and the peak value were two times larger than that of W. This result can be explained by the formation of the

charcoal barrier on the wood surface, which prevents the under-layer wood from contacting O_2, leading to the incomplete combustion of wood. The increase of COPR could cause a serious threat to people's lives. When H4A was added with APP, the large COPR peak disappeared (Fig. 9). This suggested that H4A zeolite can inhibit the emission of CO, which is of great importance for saving a human life in a fire disaster. The second COPR peak of W + APP + H4A was smaller than that of W + APP + H4A. This result suggests that H4A zeolite was more effective than 4A zeolite in reducing the COPR when the APP content is low. The COY of W was increased from 0.045 kg·kg^{-1} to 0.054 kg·kg^{-1} for W + APP, while it was reduced by about 50% with the addition of H4A zeolite (COY of W + H4A: 0.023 kg·kg^{-1}), and for W + APP + H4A, the COY was close to that of W + H4A. Therefore, a small amount of H4A zeolite (3.33 wt% of wood flour) is enough to eliminate the CO yield produced by twice as much APP as zeolite (6.67 wt% of wood flour).
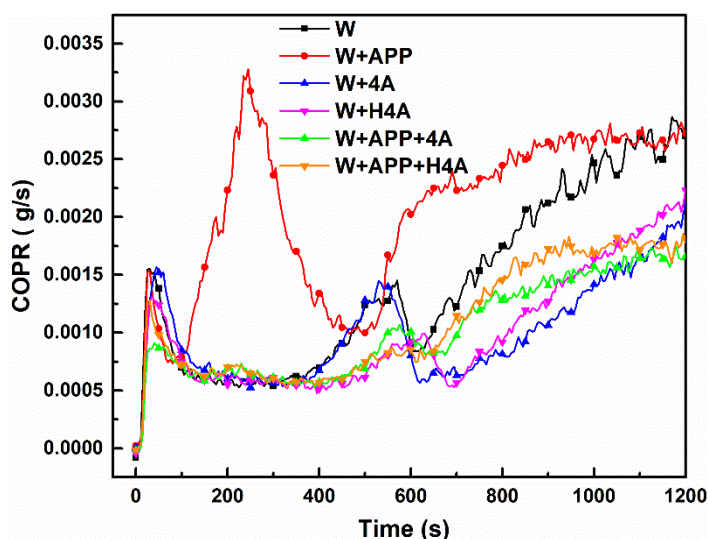
Fig. 9. The CO production rate (COPR) curves of differently treated samples

It is worth mentioning that through the experiments of this present study are tentative and limited because of the low APP content, the results of this research may provide valuable inspirations for the improvement of other fire-retardant systems, to investigate the in-depth synergistic effect of H4A zeolite and APP, more systematic studies will be done in the authors' future work.

Fire Retardant Mechanism of H4A Zeolite for Wood

The results of TG and cone calorimetry test demonstrated that H4A zeolite improved the fire retardancy of wood, and it exhibited a better inhibiting effect on smoke and CO production compared with 4A zeolite.

With hierarchical porosity, the microporous structures in H4A zeolite may act as the physical barrier to slow down the transmit rate of the heat and oxygen into wood with the intumescent char layer. The mesoporous structures would allow the rapid transmission of reactive molecules (Gueudré *et al.* 2014), accelerate the formation of the carbonaceous residue.

Furthermore, the Na$^+$ ions within the framework of H4A zeolite could affect the pyrolysis of wood toward the path of char formation (Soares *et al.* 1998), which leads to the formation of more residue. The framework of zeolite may interact with APP and

generate Si-O-P bonds to strengthen the char layer (Yan *et al.* 2017).

The unique porosity of H4A zeolite may also reduce the smoke and CO production through physical absorption. Large aperture size and pore volume which made this process more efficient. As a consequence, the fire retardancy of APP treated wood was improved, and the fire toxicity was reduced significantly. However, the exact role of mesopores of H4A zeolites on reducing the fire toxicity, *i. e.*, how does it reduced the emission of CO, remains unclear. The gas molecules may be absorbed in the mesopores in the early stage of fire or could be catalyzed and transformed to other nontoxic compounds by the active sites within the mesopores. It would be very helpful to understand the mechanism of reducing fire toxicity by carrying out a rigorous analysis of the gas and solid products during the fire in future work.

CONCLUSIONS

1. Hierarchically porous 4A zeolite and 4A zeolite were successfully synthesized in this work. Wood composites with different compositions including W, W + APP, W + 4A, W + H4A, W + APP + 4A, and W + APP + H4A were fabricated.

2. TG results showed that H4A/4A zeolites exhibit synergistic effects on increasing the residue amount. They could facilitate the formation of char residue and improve the fire retardancy of APP treated wood.

3. According to cone calorimetry test, H4A zeolite could reduce the heat release and CO production of APP treated wood composites, and it also exhibited better performance on inhibiting the smoke production compared with 4A zeolite.

4. The microporous structures of H4A zeolite may act as a physical barrier of heat and oxygen, while the mesoporous of H4A would promote the transmission of molecules to accelerate the formation of the carbonaceous residue. Meanwhile, the Na^+ ions within the framework of H4A zeolite could affect the pyrolysis of wood toward the path of char formation. Also the zeolite framework may interact with APP to generate Si-O-P bonds to enhance the char layer. More importantly, the hierarchical porosity gives H4A good absorptive properties among smoke and CO, thus reduced the fire toxicity effectively.

ACKNOWLEDGMENTS

bioresources.com

REFERENCES CITED

Ates, F., Tophanecioglu, S., and Putun, A. E. (2015). "The evaluation of mesoporous materials as catalyst in fast pyrolysis of wheat straw," *International Journal of Green Energy* 12(1), 57-64. DOI: 10.1080/15435075.2014.889005

Besser, B., Tajiri, H. A., Mikolajczyk, G., Möllmer, J., Schumacher, T. C., Odenbach, S., Gläser, R., Kroll, S., and Rezwan, K. (2016). "Hierarchical porous zeolite structures for pressure swing adsorption applications," *ACS Applied Materials & Interfaces* 8(5), 3277-3286. DOI: 10.1021/acsami.5b11120

Bourbigot, S., Bras, M. L., Bréant, P., Trémillon, J. M., and Delobel, R. (1996). "Zeolites: New synergistic agents for intumescent fire retardant thermoplastic formulations - criteria for the choice of the zeolite," *Fire and Materials* 20(3), 145-154. DOI: 10.1002/(SICI)1099-1018(199605)20:3<145::AID-FAM569>3.0.CO;2-L

Breck, D. W. (1974). *Zeolite Molecular Sieves: Structure, Chemistry, and Use*. John Wiley & Sons, Hoboken, NJ.

Cho, K., Cho, H. S., Ménorval, L. C. D., and Ryoo, R. (2009). "Generation of mesoporosity in LTA zeolites by organosilane surfactant for rapid molecular transport in catalytic application," *Chemistry of Materials* 21(23), 5664-5673. DOI: 10.1021/cm902861y

Choi, M., Cho, H. S., Srivastava, R., Venkatesan, C., Choi, D. H., and Ryoo, R. (2006). "Amphiphilic organosilane-directed synthesis of crystalline zeolite with tunable mesoporosity," *Nature Materials* 5(9), 718-723. DOI: 10.1038/nmat1705

Deka, U., Lezcanogonzalez, I., Weckhuysen, B.M., and Beale, A. M. (2013). "Local environment and nature of Cu active sites in zeolite-based catalysts for the selective catalytic reduction of NOx," *ACS Catalysis* 3(3), 413-427. DOI: 10.1021/cs300794s

Demir, H., Arkış, E., Balköse, D., and Ülkü, S. (2005). "Synergistic effect of natural zeolites on flame retardant additives," *Polymer Degradation and Stability* 89(3), 478-483. DOI: 10.1016/j.polymdegradstab.2005.01.028

Diniz, O. L. (2010). "Flame retardant for wood application," U. S. Patent No. 12/566,970.

Fu, W., Liu, T., Fang, Z., Ma, Y., Zheng, X., Wang, W., Ni, X., Hu, M., and Tang, T. (2015). "High activity and stability in the cross-coupling of aryl halides with disulfides over Cu-doped hierarchically porous zeolite ZSM-5," *Chemical Communications* 27, 5890-5893. DOI:10.1039/C4CC10417J

Gamliel, D. P., Cho, H. J., Fan, W., and Valla, J. A. (2016). "On the effectiveness of tailored mesoporous MFI zeolites for biomass catalytic fast pyrolysis," *Applied Catalysis A: General* 522, 109-119. DOI: 10.1016/j.apcata.2016.04.026

Gueudré, L., Milina, M., Mitchell, S., and Pérez-Ramírez, J. (2014). "Superior mass transfer properties of technical zeolite bodies with hierarchical porosity," *Advanced Functional Materials* 24(2), 209-219. DOI: 10.1002/adfm.201203557

ISO 5660-1 (2015). "Reaction-to-fire tests - Heat release, smoke production and mass loss rate - Part 1: Heat release rate (cone calorimeter method) and smoke production rate (dynamic measurement)," International Organization for Standardization, Geneva, Switzerland.

Jiang, J., Li, J., and Gao, Q. (2015). "Effect of flame-retardant treatment on dimensional stability and thermal degradation of wood," *Construction and Building Materials* 75(30), 74-81. DOI: 10.1016/j.conbuildmat.2014.10.037

Jiang, J., Li, J., Hu, J., and Fan, D. (2010). "Effect of nitrogen phosphorus flame

retardants on thermal degradation of wood," *Construction and Building Materials* 24(12), 2633-2637. DOI: 10.1016/j.conbuildmat.2010.04.064

Kim, J., Lee, J. H., and Kim, S. (2012). "Estimating the fire behavior of wood flooring using a cone calorimeter," *Journal of Thermal Analysis and Calorimetry* 110(2), 677-683. DOI: 10.1007/s10973-011-1902-1

LeVan, S. L. (1984). "Chemistry of fire retardancy," in: *The Chemistry of Solid Wood*, R. Rowell (ed.), International Book Distributors, Uttarakhand, India, pp. 531-574. DOI: 10.1021/ba-1984-0207

Li, J., Zhang, J., Zhang, S., Gao, Q., Li, J., and Zhang, W. (2017). "Fast curing bio-based phenolic resins via lignin demethylated under mild reaction condition," *Polymers* 9(9), 428. DOI: 10.3390/polym9090428

Lin, J. S., Liu, Y., Wang, D. Y., Qin, Q., and Wang, Y. Z. (2011). "Poly (vinyl alcohol) / ammonium polyphosphate systems improved simultaneously both fire retardancy and mechanical properties by montmorillonite," *Industrial & Engineering Chemistry Research* 50(17), 9998-10005. DOI: 10.1021/ie100674s

Lowden, L. A., and Hull, T. R. (2013). "Flammability behaviour of wood and a review of the methods for its reduction," *Fire Science Reviews* 2(4), 1-19. DOI: 10.1186/2193-0414-2-4

Marney, D. C. O., and Russell, L. J. (2008). "Combined fire retardant and wood preservative treatments for outdoor wood applications - A review of the literature," *Fire Technology* 44(1), 1-14. DOI: 10.1007/s10694-007-0016-6

Moreno-Recio, M., Santamaría-González, J., and Maireles-Torres, P. (2016). "Brönsted and Lewis acid ZSM-5 zeolites for the catalytic dehydration of glucose into 5-hydroxymethylfurfural," *Chemical Engineering Journal* 303, 22-30. DOI: 10.1016/j.cej.2016.05.120

Naeher, L. P., Brauer, M., Lipsett, M., Zelikoff, J. T., Simpson, C. D., Koenig, J. Q., and Smith, K. R. (2007). "Woodsmoke health effects: A review," *Inhalation toxicology* 19(1), 67-106. DOI: 10.1080/08958370600985875

Pérez-Ramírez, J. (2012). "Zeolite nanosystems: Imagination has no limits," *Nature Chemistry* 4, 250-251. DOI: 10.1038/nchem.1310

Soares, S., Camino, G., and Levchik, S. (1998). "Effect of metal carboxylates on the thermal decomposition of cellulose," *Polymer Degradation and Stability* 62(1), 25-31. DOI: 10.1016/S0141-3910(97)00256-5

Spearpoint, M. J., and Quintiere, J. G. (2000). "Predicting the burning of wood using an integral model," *Combustion and Flame* 123(3), 308-325. DOI: 10.1016/S0010-2180(00)00162-0

Stec, A. A., and Hull, T. R. (2010). *Fire Toxicity,* Woodhead Publishing, Sawston, Cambridge.

Steen-Hansen, A., and Kristoffersen, B. (2007). "Prediction of fire classification for wood based products. A multivariate statistical approach based on the cone calorimeter," *Fire and Materials* 31(3), 207-223. DOI: 10.1002/fam.934

Treacy, M. M. J., and Higgins, J. B. (2007). *Collection of Simulated XRD Powder Patterns for Zeolites*, Fifth (5th) Revised Edition, Elsevier, New York, NY.

Vermeiren, W., and Gilson, J. P. (2009). "Impact of zeolites on the petroleum and petrochemical industry," *Topics in Catalysis* 52(9), 1131-1161. DOI: 10.1007/s11244-009-9271-8

Wang, L., Toppinen, A., and Juslin, H. (2014a). "Use of wood in green building: A study of expert perspectives from the UK," *Journal of Cleaner Production* 65, 350-361.

DOI: 10.1016/j.jclepro.2013.08.023

Wang, M., Wang, X., Li, L., and Ji, H. (2014b). "Fire performance of plywood treated with ammonium polyphosphate and 4A zeolite," *BioResources* 9(3), 4934-4945. DOI: 10.15376/biores.9.3.4934-4945

Wang, T., Yang, S., Sun, K., and Fang, X. (2011). "Preparation of Pt/beta zeolite–Al2O3/cordierite monolith for automobile exhaust purification," *Ceramics International* 37(2), 621-626. DOI: 10.1016/j.ceramint.2010.09.035

Wang, W., Zhang, W., Chen, H., Zhang, S., and Li, J. (2015). "Synergistic effect of synthetic zeolites on flame-retardant wood-flour/polypropylene composites," *Construction and Building Materials* 79, 337-344. DOI: 10.1016/j.conbuildmat.2015.01.038

Wu, J., Wang, M., and Guo, H. (2017). "Synergistic flame-retardant effects of different zeolites on intumescent fire-retardant coating for wood," *BioResources* 12(3), 5369-5382. DOI: 10.15376/biores.12.3.5369-5382

Yan, L., Xu, Z., and Wang, X. (2017). "Influence of nano-silica on the flame retardancy and smoke suppression properties of transparent intumescent fire-retardant coatings," *Progress in Organic Coatings* 112, 319-329. DOI: 10.1016/j.porgcoat.2017.07.017

Yunchu, H., Peijang, Z., and Songsheng, Q. (2000). "TG-DTA studies on wood treated with flame-retardants," *Holz als Roh- und Werkstoff* 58(1-2), 35-38. DOI: 10.1007/s001070050382

Zorpas, A. A., Constantinides, T., Vlyssides, A. G., Haralambous, I., and Loizidou, M. (2000). "Heavy metal uptake by natural zeolite and metals partitioning in sewage sludge compost," *Bioresource Technology* 72(2), 113-119. DOI: 10.1016/S0960-8524(99)00110-8